Journal of Power Sources 196 (2011) 7899–7916

Contents lists available at ScienceDirect

Journal of Power Sources

journal homepage: www.elsevier.com/locate/jpowsour

Review

Analysis of multi-phase transport phenomena with catalyst reactions in polymer electrolyte membrane fuel cells – A review

Munir Ahmed Khan*, Bengt Sundén, Jinliang Yuan

Department of Energy Sciences, Box 118, Faculty of Engineering, Lund University, 22100, Lund, Sweden

ARTICLE INFO

Article history:
Received 29 January 2011
Received in revised form 26 March 2011
Accepted 19 April 2011
Available online 17 May 2011

Keywords:
PEMFC
Multi-phase
Macroscopic models
Modeling discrepancies
Meso-scale modeling
Validation

ABSTRACT

A review is presented for two-phase modeling approaches to study various transport processes and reactions in polymer electrolyte membrane (PEM) fuel cells along with some experimental work. It has been noted that water management is still one of the least accurate modeled phenomena. The lackness in complete descriptive models for water management inside PEM fuel cells can be attributed to the complexity of the phenomena, lack of empirical or measured data and non-availability of apt governing equations.

Another discrepancy found in present models is the proper validation of the numerical work as it has been observed that mere comparison with V–I curve can sometimes lead to misguided conclusions. Additionally, keeping in mind the multi-scale nature of a PEM fuel cell, application of the Lattice Boltzmann (LB) method has also been reviewed in this work and it was noticed that LB methods offer bright perspective at meso-scale by incorporating details of local structure. Furthermore, a brief description of the catalyst layer models is also presented with some technological developments at nano-scale to improve the physio- and electro-chemical properties. A test case for a 2D PEM cathode is also simulated for different operating voltages to predict the water saturation effects.

Contents

* Corresponding author. Tel.: +46 46 222 4105; fax: +46 46 222 4717.
E-mail address: Munir.Khan@energy.lth.se (M.A. Khan).

0378-7753/$ – see front matter © 2011 Elsevier B.V. All rights reserved.
doi:10.1016/j.jpowsour.2011.04.040

1. Introduction

Fuel cells have become a pivot of energy research activities in the present decade. With increasing energy demands and depleting organic fuels, a need for sustainable and efficient energy production had never been felt so urged as of today. With many different alternative proposals provided by the scientific and engineering communities, fuel cells stand a biased position because of their high efficiency with a byproduct of low to zero greenhouse gas emissions and abundance of fuel availability. Among many different types of fuel cells, polymer electrolyte membrane (PEM) fuel cells have taken the lead because of their low operating parameters, cost effectiveness, high current density and compactness for mobile applications [1–3].

An outlook of PEM fuel cells has a deceptive presentation as being very simple and straightforward piece of equipment in both making and service. However, turning around the coin indicates that they are not more simpler than any other energy production devices, and quantifying and measuring all the processes and phenomena inside PEM fuel cells is not only impossible [3] but the highly reactive environment also makes it quite difficult to measure even simple parameters like temperature, pressure, electric potential and species gradients, etc. [4]. In recent years, much critical work has been performed in various disciplines of PEM fuel cells from basic electro-chemistry to design of stacks, but, numbers of issues are still pending and need to be resolved for commercial viability and many improvements are deemed necessary to remove the big question mark about the future of PEM fuel cells as an alternative energy production unit.

It has been well established that cathode performance is one of the key issue still under intensive investigation without any proper remedy yet proposed [5]. The important factors affecting the cathode performance are [6];

- slow reaction kinetics,
- formation of liquid water and water management,
- thermal management.

In PEM fuel cells, the oxygen reduction reaction (ORR) is the rate determining step for the overall electro-chemical reaction. Despite the active research in improving the physio-chemical behavior of the cathode catalyst it has been determined that the ORR is about four to six times slower to the hydrogen oxidation reactions (HOR) occurring at the anode [6,7]. Formation of liquid water at the cathode of PEM fuel cell is an another major contributor to the under-grade performance of the cathode especially at high loads by blanketing the reaction sites by making them unavailable for three-phase contact.

Different processes contributing to water formation or removal during the operation of PEM fuel cells at the cathode are; [8] (the negative mechanisms in water source represent removal of water content while increase in water quantity inside the fuel cell is represented by the positive sources);

- oxygen reduction reaction (positive)
- electro-osmotic diffusion (positive)
- condensation of water vapors (positive)
- back diffusion (negative).
- evaporation (negative).

The ion transport in form of H_3O^+ uses water molecules as a carrier from anode to cathode of a PEM fuel cell. It is estimated that

Nomenclature

A_{agg}	Effective agglomerate surface area ($m^2\ m^{-3}$)
$C_{O_2}^{bulk}$	Local O_2 concentration ($mol\ m^{-3}$)
D_b, D_i	Bulk diffusivity of species i ($m^2\ s^{-1}$)
D_k	Knudsen diffusivity ($m^2\ s^{-1}$)
D_{eff}	Effective diffusivity of species ($m^2\ s^{-1}$)
F	Faraday's constant
h_v	Interstitial heat transfer coefficient ($W\ m^{-3}\ K^{-1}$)
K	Permeability (m^2)
k	Reaction rate constant (s^{-1})
k_{con}	Condensation rate constant (s^{-1})
k_{eva}	Evaporation rate constant ($Pa\ s^{-1}$)
k_n	Knudsen number
l	Characteristic flow dimension (m)
i	Current density ($A\ m^{-2}$)
M_i	Molecular weight of species ($kg\ mol^{-1}$)
P_c	Capillary pressure (Pascals)
R	Universal gas constant ($J\ mol^{-1}\ K^{-1}$)
r	Radius (m)
X	Species mass fraction
z	Number of electrons consumed per mole of reactant

Greek Letters

δ_{film}	Thickness of electrolyte film covering an agglomerate (m)
ε_{agg}	Proportion of electrolyte in agglomerate
ε	Porosity of material
ϕ	Theile's modulus
λ	Mean free path of molecules (m)
ρ	Density ($kg\ m^{-3}$)
σ	Surface tension ($N\ m^{-1}$)

Subscripts and superscripts

agg	Agglomerate
c	Catalyst layer
eff	Effective
f	Fluid phase
i	Species
Pt	Platinum
s	Solid phase
v	Void space

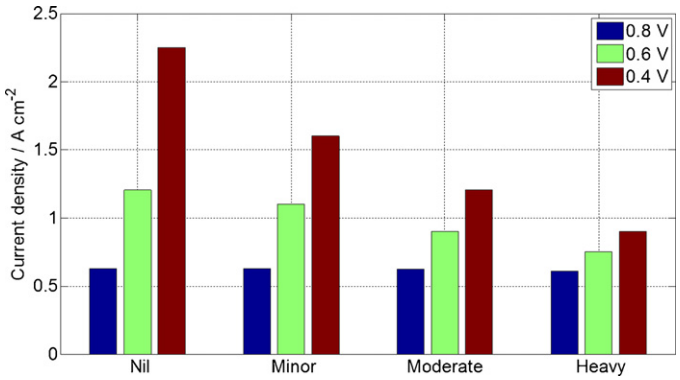

Fig. 1. Comparison of current density at different voltages with various levels of water flooding in the porous media.

one to five molecules of water are dragged per proton migration from anode to cathode side [9,10]. Similarly, along the production of water due to ORR, condensation of water vapors also proves to be handy in formation of liquid water if the vapor quantity exceeds its saturation limit in the inlet air supply to PEM fuel cell. The anti-measures for the formation of water are back diffusion resulting due to the concentration difference in water across the anode and the cathode, and the evaporation of liquid water due to high inlet temperature or saturation pressure. If the formation rate of water is not balanced by the removal rate, accumulation of liquid water occurs at the cathode resulting in water flooding. This non-equilibrium of production and removal is known to cause major performance hold ups to PEM fuel cells in terms of efficiency, stability and reliability [11,12].

Although, water formation has been labeled as one of the performance defectors in PEM technology, many processes inside the PEM fuel cells are itself highly water dependent. As already stated, the proton migration from anode to cathode i.e., the protonic conductivity of the membrane material incorporated in low temperature (<100 °C) PEM fuel cells, is highly water dependent. The dryness of the membrane will render it from low to zero conductivity causing major suffering in performance by considerably increasing the ohmic losses [10]. To ensure proper hydration of the membrane, a balance between inlet humidification and evaporation rate has to be maintained. So, overall, the formation and removal rate of water has to be closely monitored and balanced not only to avoid flooding of the cathode but also for proper wetting of the membrane.

As discussed above, the water management problem is one of the major issues related to the optimum performance and stable operation in PEM fuel cells. A comparison of different water flooding levels is given in Fig. 1 for the current produced for each operating voltage. As it can be seen that, when the water flooding increases, the maximum current density for a specific voltage decreases considerably. At low current densities, the current density is almost the same for all levels because at such low operating conditions the reaction rate is quite low and water formation due to both ORR and electro-osmatic drag is not significant but at higher levels of water flooding there is decrease of almost 80% in the current density produced at 0.4 V.

Many reviews of PEM fuel cell modeling have been published by, e.g., Biyikoglu [13], Cheddie and Munroe [4], Wang [14], Haraldsson and Wipke [15], Siegel [3] and Mench [16] etc. Most of the reviews were conducted for general models related to conservation equations, spatial dimensions and level of model complexity. The present work is limited to two-phase flow models as the water management still remains one of the key issues for PEM fuel cells. Also, a brief insight will be provided for micro-scale model developments in PEM fuel cell both in terms of Computational Fluid Dynamics (CFD) analysis and catalyst layer modeling.

2. Classification of models

Because of vast diversity of technologies incorporated in a single PEM fuel cell, it is quite difficult to classify and fix a certain model to a particular subclass, e.g., even in CFD modeling, equations of voltages need to be solved for electro-chemical reaction rates besides verification of modeling. Similarly, electrical, heat and species transport losses need to be accounted for the simplest of the models. Apart from this, anisotropy of material properties extend the models floating in various domains.

Many authors have already attempted to classify PEM fuel cell models according to their own dominions, e.g. Khan [8] has classified PEM models based on thermal analysis (isothermal and non-isothermal), flow (single- or two-phase) and the electro-chemical model used to simulate the reactions in the catalyst layer. Similarly, Cheddie and Munroe [4] have categorized PEM fuel cell models based on modeling approach used, i.e., analytical models, semi-empirical models and mechanistic models. Analytical models represent the simplest of all as many simplifying assumptions are employed that results in approximate analytical voltages versus the current density relationships [17–19]. In semi-empirical models, empirically determined properties are used with theoretical differential and algebraic equations [20], while, mechanistic models have been more popular in modeling in which the differential equations are derived from physics and electro-chemistry of the internal phenomena in PEM fuel cells [21–23].

Siegel [3] has categorized PEM fuel cell models in his review article based on geometric constraints of the models from one to three dimensions. Classification based on the length scales of the computational domains has also been proposed by Mench [16] and Djilali and Sui [24]. The length scale varies from the molecular level to full system size with different purposes and outcomes. The molecular models deal more with an attempt to model transport of charge, mass and heat to interpret the limitations that significantly affect the overall performance of fuel cells [16,25–28] whereas, system or stack models deal more with efficiencies, losses and geometric limitations of the complete energy system [19,29–38].

3. Macroscopic models and challenging issues

Basically, a fuel cell is an electro-chemical device that converts the chemical energy into the electrical energy without any intermediating assistance or device. Main components of a single PEM fuel cell can be listed as;

- membrane
- catalyst layer
- gas diffusion layer (GDL, also known as porous transport layer, PTL)
- current collectors
- flow channels.

Membrane is the parting component between anode and cathode sides of the fuel cell while catalyst layer, GDL and current collectors on either side of the membrane constitute the electric poles of the cell. Fuel (hydrogen) is fed to the anode side of the fuel cells, and is distributed on the catalyst layer by the GDL to produce electrons and protons according to Eq. (1);

$$2H_2 \rightarrow 4H^+ + 4e^- \quad (1)$$

Electrons are forced to flow through the external path, while, protons migrate internally through membrane by selecting such a

Table 1
Governing equations for PEM fuel cell models and applicable component of PEM fuel cell.

Equation			Region of application	Remarks
1.	Continuity	$\nabla \cdot (\rho \vec{v}) = S_m$	CL, GDL, flow channels	X
2.	Momentum	$\nabla \cdot (\rho \vec{v}\vec{v}) = -\nabla p + \nabla \cdot \left(\bar{\bar{\tau}}\right) + \rho \vec{g} + \vec{F}$	CL, GDL, flow channels	X
3.	Species transport	$\nabla \cdot \left(\rho \vec{v} X_i\right) = -\nabla \cdot \vec{J}_i + R_i + S_i$	CL, GDL, flow channels	X
4.	Energy equation	$\nabla \cdot \left(\rho c_p T_f\right) = \nabla \cdot \left(k_{eff} \nabla T_f\right) + S_f 0 = \nabla \cdot \left(k_{\text{eff}} \nabla T_f\right) + S_s$	All regions	One equation or LTNE approach
5.	Electric potential	$-\nabla \cdot (\sigma_s \nabla \phi_s) = S_{\phi_s} - \nabla \cdot (\sigma_m \nabla \phi_m) = S_{\phi_m}$	All regions except flow channels	Solid phase and membrane phase potential
6.	Secondary phase	$\nabla \cdot \left(\rho_l \vec{V} s\right) = R_w$	All regions except current collectors	Multi-phase models in gas channels, water saturation equation in CL and GDL, water flux in membrane

material that poses high electron resistivity and proton conductivity (the detailed structure of membrane materials can be found in [39]). Oxygen and charged entities (e^- and H^+) transported from anode combine at the cathode to produce water as a product.

$$O_2 + 4H^+ + 4e^- \rightarrow 2H_2O \quad (2)$$

Eqs. (1) and (2) represent the half-cell reactions of anode and cathode sides respectively and are catalyzed with platinum present in the catalyst layer on either sides.

With advances in computer technologies and enhanced speeds, CFD modeling approach has provided scientists and engineers with internal anatomy of fundamental processes of a PEM fuel cell [8]. To date many models for PEM fuel cells have been proposed with varying complexity and texture, however, there is no single complete model that would effectively and efficiently explain and chalk out the phenomena altogether. Nevertheless, for a descriptive model of PEM fuel cell, Biyikoglu [13] has outlined basic conditions or processes, inclusion of which can result in a much descriptive model, given as;

- balanced current distribution
- control of water flow
- efficient removal of liquid water
- removal of excessive heat.

Although, basic outline, as explained above, is very useful in developing a CFD model of PEM fuel cells, still ultimate and complete PEM fuel cell model is quite difficult to achieve due to inherent limitations of the analysis and outputs desired. The main limitations still blocking the researchers from attaining the ultimate goal of completeness, as given by Mench [16], are the inclusion of the physico-chemical phenomena, knowledge of the transport phenomena, computational power and proper validation of the models.

The governing equations used in PEM fuel cell models are given in Table 1 with applicable component regime and the source terms for each governing equations are given in Table 2 for a typical PEM fuel cell CFD model. The detailed description of the governing equations along with nomenclature and source term evaluation for all the fundamental processes can be found in [8], here some of the important and usually ignored factors are outlined.

3.1. Anisotropy of physical properties

Regarding the porous media of PEM fuel cells, it is revealed that it comprises of fibrous media that has significant anisotropy due to its orientation of the fibers. Due to this, the in-plane and through-plane properties vary significantly [40,41]. The major properties influenced by anisotropy are;

- species transport
- heat conduction
- electrical conduction
- water saturation.

For species transport in the porous media, most of the authors use Bruggeman's correction factor. However, accounting for anisotropy, the effective diffusion coefficient is a tensor rather than scalar quantity. As presented by Nam and Kaviany [42], the effective diffusion coefficient in the porous media in PEM fuel cells is better depicted by using percolation theory, given as;

$$D_g^{\text{eff}} = f(\varepsilon) \times D_g^i \qquad f(\varepsilon) = \varepsilon \left(\frac{\varepsilon - \varepsilon_p}{1 - \varepsilon_p}\right)^{\alpha} \qquad \alpha = \begin{cases} 0.521 & \text{in-plane} \\ 0.785 & \text{through-plane} \end{cases} \quad (3)$$

where ε_p is the percolation critical value and has been reported to be 0.11 and 0.13 by Pharoah et al. [43] and Liu and Wang [44], respectively. The results produced by the anisotropic diffusion coefficient reveal that the gas flow is much higher in in-plane direction than through-plane directions suffocating the reaction sites in the catalyst layer. Similarly, the thermal conductivity of the porous media is almost 14 times more in in-plane direction and temperature differential of more than 5 °C in through-plane was observed in work by Pasaogullari et al. [41]. Meng [40] has also suggested anisotropic electrical conductivity of the porous media and a difference of more than 2000 (s m^{-1}) was reported to exist in in-plane and through-plane directions. Similarly, apart from anisotropic effects, the experimental and CFD modeling results also vary as the temperature gradients observed are much lower while simulated numerically using the parallel resistance approach, given as [43];

$$k_{\text{eff}} = \varepsilon k_v + (1 - \varepsilon) k_s \quad (4)$$

Table 2
Source terms for governing equations.

Equations	Source term	Gas diffusion layer (GDL)	Catalyst layer (CL)
Momentum	$\dot{m}_{\text{ORR},O_2}$	0	$-\frac{M_{O_2}}{4F} \nabla \cdot i$
	$\dot{m}_{\text{ORR},H_2O}$	0	$\frac{M_{H_2O}}{2F} \nabla \cdot i$
	$\dot{m}_{\text{Phase}}$	Eq. (12)	Eq. (12)
Energy	$\dot{q}_{\Omega}$	$\frac{i_s^2}{\sigma_{s,\text{eff}}}$	$\frac{i_s^2}{\sigma_{s,\text{eff}}} + \frac{i_m^2}{\sigma_{m,\text{eff}}}$
	$\dot{q}_{\text{phase}}$	$\dot{m}_{\text{phase}} \times h_{fg}$	$\dot{m}_{\text{phase}} \times h_{fg}$
	$\dot{q}_{it}$	$h_v(T_s - T_f)$	0
	$\dot{q}_{\text{ORR}}$	0	$(\phi_m - \phi_s) \times \nabla \cdot i$
Charge	S_{ϕ_s}	0	$\nabla \cdot i$
	$S_{\phi m}$	0	$-\nabla \cdot i$

where k_s and k_v are solid and void thermal conductivities, respectively. The conduction of heat, as predicted by Eq. (5) is assumed to travel either through void or solid regions contrary to combined path. Pharoah et al. [43] suggested a novel approach by stacking the solid and void regions so that all of the heat is passed through combined solid and void regions termed as the network resistance approach.

$$k_{\text{eff}} = \frac{k_s k_v}{\varepsilon k_s + (1-\varepsilon)k_v} \tag{5}$$

The heat transport predicted by utilizing the thermal coefficient as given by Eq. (5) is approximately the same as encountered in reality [43].

Similarly, most of the two-phase models use Leverett function to simulate the water flow in PEM fuel cells [8,41,45]. This function is highly dependent on the permeability of the porous media which in turn is actually anisotropic in nature, as given by [41];

$$j_x = C_1 k_{xx} \quad \text{and} \quad j_y = C_2 k_{yy} \tag{6}$$

where j_x and j_y are the mass flux of liquid water in respective directions, k_{xx} and k_{yy} represent the anisotropic permeability in the principle directions of the porous media. It is found that water saturation levels are always higher in this case, thus reducing the overall performance of the PEM fuel cells [41].

3.2. Local thermal non-equilibrium (LTNE) approach

The condition to use one equation model for heat transport or local thermal equilibrium (LTE) is only valid when the temperature difference between the fluid and the solid phases of the porous electrode is much lower than the overall system temperature difference. Since, PEM fuel cells are low operating temperature devices, the magnitude of both the temperature differences between phases and the overall temperature difference is almost same, given mathematically as [46];

$$\text{O}\left|\frac{\Delta T_{\text{loc}}}{\Delta T_{\text{sys}}}\right| \sim 1 \tag{7}$$

where ΔT_{loc} is local temperature difference between the phases while ΔT_{sys} represents the overall system temperature difference. In LTNE approach both the phases i.e., void and solid portions of the porous media are represented by separate equations and interlinked through a volumetric heat transfer coefficient h_v ($\text{W m}^{-3}\,\text{K}^{-1}$). The exact value of h_v has not been measured yet but experimental results obtained for the aluminum foam ranging from 3×10^4 to 1.5×10^5 ($\text{W m}^{-3}\,\text{K}^{-1}$) [46] has been used by some authors. To date many researchers have implemented LTNE approach in both single phase and two-phase flow regimes but limiting the geometry to 2D only [8,23,46–49]. Since many parameters in PEM fuel cell are temperature dependent, LTNE approach to 3D models need to be evaluated and compared with the local thermal equilibrium or the so-called one equation models.

3.3. Knudsen diffusion

Usually effective diffusion coefficient modified by Bruggeman's correction is employed in species transport of oxidants and fuels in the porous media of the PEM fuel cells. However, the texture of porous media is very complex and the relative influence of ordinary diffusion or Knudsen diffusion on species transport is governed by the pore geometry [50]. According to Malek and Coppens [51], for the media with pore dimensions of 2–50 nm, Knudsen diffusion is the predominant transport mechanism which results from the collision of gas molecules with the pore walls instead of intra-molecular collision (Brownian motion). The Knudsen diffusion coefficient for CFD calculations can be used in the form of [52];

$$D_k = \frac{2}{3} r_e \sqrt{\left(\frac{8RT}{\pi M_i}\right)} \tag{8}$$

The effective diffusion coefficient based on both bulk diffusion and Knudsen diffusion can be calculated as [53];

$$\frac{1}{D_{\text{eff}}} = \left(\frac{1}{D_b} + \frac{1}{D_k}\right) \times f(\varepsilon) \tag{9}$$

where $f(\varepsilon)$ is the correction factor for the porous medium and can be evaluated according to Eq. (3).

3.4. Modeling software and solutions

With in-house self-developed and open-source CFD models, many commercial software products are available in the market that have proved to be very efficient and robust. Regardless of inherited disadvantage of limited freedom in equation manipulation and controls, many researchers have opted for commercial software products as prime CFD tool. Among many, the most commonly used are FLUENT®, COMSOL®, STAR-CD® and CFD-ACE+®, and the contribution of each in CFD modeling is shown pictorially in Fig. 2 [3].

ANSYS® Fluent® [54] is a powerful commercial software available in the market offering sophisticated numerics and robust formulations including a pressure-based segregated and coupled solvers, and a density based solver technique to ensure optimum and reliable results. It is well suited for a number of complex physical models utilizing unstructured meshes both for 2D and 3D cases based on finite volume method (FVM). Meshes can be created using ANSYS® meshing products or other robust products like ICEM® and GAMBIT®. To further enhance the flexibility of model variant situations, Fluent® provides the use of user-defined-functions (UDFs) that help to tailor the model to specific needs or requirements. With the increase in demands for fuel cells CFD analysis, an add-on is provided to simulate typical PEM fuel cells. In this module, the two-phase flow in the porous media is solved using the Leverett function while in gas channels it is assumed that both gases and water flow with the same velocity in form of fine mist. The potential equations for both solid and membrane phases are also solved to get the inside distribution of electric and ionic currents, respectively. The additional capability of Fluent® software to solve user-defined-scalars provides a handy tool to simulate most of the internal phenomena occurring inside PEM fuel cells. Fluent also offers extended post-processing tool and provides provision to export the data to other post-processing software solutions. In order to simulate the electro-chemical reactions, a choice is also provided to select either Tafel formulation or the advanced Butler–Volmer kinetics. Furthermore, to enhance the flexibility of the PEM fuel cell module, it is also made possible to specify requirement based specific functions and models through a modifiable source code.

COMSOL Multiphysics® [55] is another commercial software product available widely for simulating fluid flow incorporating finite element method (FEM) with stiff chemistry solvers. This software also offers flexible equation based modeling with various degrees of mesh complexity. The user can also include partial differential equations (PDEs) using various formulations and the software can automatically detect the best possible solver and settings for a particular problem along with manual tuning. Since fuel cells have become a beacon of future power, an add-on module has been released in the latest version V4. Compared to Fluent® in which add-on module is only available for PEM and solid oxide fuel cells (SOFCs), COMSOL®, on the other hand, also supports alkaline, molten carbonate and direct methanol fuel cells. As far the

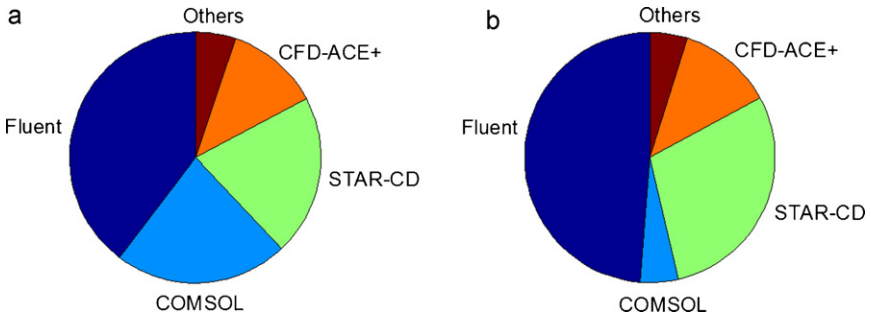

Fig. 2. Comparison of commercial and non-commercial software used for PEM fuel cell CFD. (a) Trend of software used for CFD modeling in overall; (b) trend of software used for 3D modeling. (For commercial software, data is adopted from Siegel [3]).

mesh generation for COMSOL applications is concerned, a built-in geometry and mesh generator is available in standard package with sound post-processing facility.

STAR-CD® [56] and CFD-ACE+® [57] are other finite volume based CFD software products also commercially available. Both products have strong parallel computing capabilities with aptitude to handle complex geometries including multiphysics modules for PEM fuel cells that can be handled quite easily. CFD-ACE+® also offers the facility to carryout stress and strain analysis within the PEM fuel cells. Alongside licensed commercial software, OpenFOAM is open code software with pre-developed modules for simulating complex multiphysics problems with good pre- and post-processing utilities also based on finite volume technique. Additionally, meshes from other software can also be imported and manipulated. The advantages offered by OpenFOAM are that users can extend or create own libraries and manipulate the solver to suit the demands. Although no fuel cell modules are provided built-in but with good coding knowledge, efficient and robust models can be developed that can handle a variety of problems [3].

4. Two-phase models

Water management inside PEM fuel cell is of paramount importance because operation of a PEM fuel cell is highly dependent on the water content as protonic conductivity of the membrane material, typically used for low operating temperature fuel cells, is highly dependent on the amount of water present [39,58]. Decrease in water content can cause dry out of membrane and reduce protonic migration, thus, it is very essential that the membrane remains fully hydrated all the times. However, excessive water inside PEM fuel cell can lead to clogging of channels [59,60], and, flooding of the catalyst layer [59,61,62] and long term liquid water accumulation inside PEM fuel cell is also one of the major contributor to the degradation of the catalyst and its carbon support material, ionomer poisoning and hydrophobicity loss [63]. In this section, an insight into selected two-phase models is presented with a summarized outline in Table 3. The list presented here is not an exhausted one but it has been made to include different variety of two-phase CFD models used in the research society in last 10 years.

4.1. CFD modeling review

He et al. [64] performed multi-phase simulations of PEM fuel cell. In their model, the droplet size of water was taken as the prime parameter to study the multi-phase flow. A multi-phase mixture model was applied to a 3D geometry. The interaction effect between the phases was studied by considering droplet size, drag coefficient, Reynolds number, velocity and droplet relaxation time. The equation for calculating the droplet size was adapted from Zhang et al. [60]. The advantage associated with this model is that it includes the effect of liquid water removal from the channels of PEM fuel cell. In this work all the simulations were performed on a commercial CFD software.

Yuan and Sundén [65] also developed a 3D model to understand the effect of liquid water on cell performance. The model presented is a half-cell model considering cathode only because of its slower kinetics. The electro-chemical reactions were modeled to occur in a thin layer while simulating the flow in GDL and the channels. The salient features of this work were the use of combined thermal boundary conditions and mass transfer along with the effect of saturation on current density profile. The calculation domain was discretized by finite volume method and a combination of uniform and non-uniform grid spaces. The simulations were performed using an in-house CFD code. The saturation was evaluated based on the saturation pressure and the local temperature of the flow. Wang et al. [66] also proposed a two-phase model of PEM fuel channels to simulate the flow of liquid water and gaseous reactants. Darcy's law and multi-phase mixture model was employed for estimation of the key parameters such as overall pressure drop and liquid saturation profile along the channel and flow analogy to random porous media. The physical model used in this work consisted of a single straight channel for the cathode side. Fully or partially humidified air feed was used at the inlet and the water produced as a result of electro-chemical reactions was injected into the channel along its length.

He et al. [21] performed a 2D analysis of a PEM fuel cell with interdigitated flow field by solving two-phase, multi-component transport equations. Darcy law was used to simulate the gas phase transport, while for liquid water, both the capillary pressure and the shear force between the two-phase was considered as the prime transport mechanisms. The modeled region consisted of a GDL and the current collector. The electro-chemical reactions were assumed to occur at the boundary of GDL, i.e., a thin layer model was used.

Le and Zhou [67] presented a general model of PEM fuel cell which accounted for fluid flow, heat transfer, species transport, electro-chemical reactions and water saturation. Detailed thermo-electro-chemistry studies were carried out on a 3D geometry where saturation effects were evaluated with explicit gas–liquid interface tracking using VOF multi-phase model. Commercial software Fluent® was employed for simulations and calculations. In this model, all the components of a complete single fuel cell unit were included to broaden the results scope and the effect of liquid saturation along with porous media was also studied. The flow field design employed in this model was the serpentine flow field. Initially, water droplets of 0.4 mm were assumed suspended in the flow field and their behavior was studied at different time steps at an operating voltage of 0.5 V.

Hwang [23] has also developed a 2D model of PEM fuel cell in which two separate momentum equations were applied for gaseous and liquid flow. Heat distribution was simulated using the LTNE approach that considered separate energy equations for fluid and solid components in the GDL. Also, irreversible heat generation

Table 3
Summarized features of the review articles.

	Author	Chemical kinetics	Saturation equation	Model validation	Geometry	Major conclusions
1.	He et al. [64]	Butler–Volmer	$\frac{\partial}{\partial t}(\varepsilon\rho_l s) + \nabla\cdot\left(\rho_l \frac{Ks^3}{\mu_l}\frac{d}{ds}(p_c)\nabla s\right) = S$	Experimental Fluent PEM module	3D	Large water droplets increase saturation Liquid water hinders heat transfer in gas diffusion layer and catalyst layer causing hot spots Co-flow pattern is disadvantageous for PEM fuel cells as compared to counter-flow pattern
2.	Yuan and Sundén [65]	Tafel equation	$s = \frac{\rho\phi_w - \rho_g\phi_{wv}}{\rho_{wl} - \rho_g\phi_{wv}}$	X	3D Cathode only	The non-uniformity in the current distribution resulted because of uneven distribution and transport of the reacting air Higher saturation levels resulted in low current densities Low-operating parameters (temperature and humidity) also decreases the current density
3.	He et al. [21]	Tafel Equation	$v^l = fv^g - D_c\nabla s$	Experimental	2D Cathode only	In interdigitated flow fields along with evaporation of liquid water, the liquid water transport also acts as water removal mechanism Higher oxygen flow improves the reactant transport The thickness of electrodes effects the current density For interdigitated flow fields, a shorter rib dimensions improves the performance
4.	Le and Zhou [67]	Butler–Volmer	$\frac{\partial}{\partial t}(\varepsilon s_l\rho_l) + \nabla(s_l\rho_l\vec{v}) = S$	Visual	3D	Liquid droplets cause high pressure drop regions The turning areas of the serpentine flow field showed increased water droplet formation causing a substantial air flow blockage The channel structure significantly influences the water distribution inside the cell High saturation causes excessive concentration losses Area under the channels give higher reaction rates However, the presence of liquid water reduced the overall temperature of the cell
5.	Hwang [23]	Butler–Volmer	$\frac{1}{\varepsilon}\nabla\cdot(\rho u_g u_g) = -\varepsilon[\nabla p_c + (\rho_w - \rho_g)g] + \nabla\cdot(\mu_w\nabla u_w) - \frac{\varepsilon\mu_w u_w}{\kappa k_{rw}}$	Experimental	2D	Increasing the current collector temperature reduces water saturation by helping evaporation.

Table 3 (*Continued*)

	Author	Chemical kinetics	Saturation equation	Model validation	Geometry	Major conclusions
6.	Senn and Poulikakos [45]	Tafel equation	$p_c = \frac{\sigma \left\lvert \cos\theta \right\rvert}{(\kappa/\varepsilon)^{1/2}} J(s)$ $J(s) = 1.417s - 2.12s^2 + 1.263s^3$	X	2D	Decreasing the dimensions of current collector width, channel width and GDL thickness improved the performance of the PEM fuel cell For small channel widths, a thin GDL performed better that thick GDL
7.	Siegel et al. [73]	Agglomerate	$\tilde{u} \cdot \nabla s = \nabla \cdot \left(D_{WL}^{cp} \nabla s \right) + S$	Experimental	2D	Liquid water has significant effect on fuel cell performance Water content in catalyst layer and transport through membrane also effect the ohmic losses and reactant transport properties in the cathode catalyst 20–40% of the liquid water is accumulated in the cathode catalyst layer
8.	Yu et al. [74]	Butler–Volmer	$\nabla \cdot (\varepsilon \rho u C_\alpha) = -\nabla \cdot J_\alpha + S$	Experimental	3D	Pure oxygen instead of inlet air increases fuel cell performance A thin PEM fuel cell has better performance characteristics than a thicker one High inlet velocity increases the current density Increasing current collector width has no prominent effect on the current density
9.	You and Liu [69,70]	Butler–Volmer	$\varepsilon \frac{\partial}{\partial t}(\rho C^\alpha) + \nabla \cdot (\gamma_\alpha \rho u C^\alpha) = \nabla \cdot (\varepsilon \rho D \nabla C^\alpha) + \nabla \cdot \left[\varepsilon \sum_k \left[\rho_k s_k D_k^\alpha \left(\nabla C_k^\varepsilon - \nabla C^\alpha \right) \right] \right] - \nabla \cdot \left[\sum_k C_k^\alpha J_k \right]$	Experimental	2D	The water content increasing along the thickness of the membrane towards the cathode indicating large water migration from anode to cathode Increasing the current increases oxygen consumption At the cathode side, the protonic current is zero at the GDL/catalyst layer interface and increases towards the catalyst/membrane interface and is higher for high current density. Similarly, the overpotential corresponds directly to the magnitude of current density

Table 3 (*Continued*)

	Author	Chemical kinetics	Saturation equation	Model validation	Geometry	Major conclusions
10.	Meng [80]	Butler–Volmer	$\nabla \cdot \left[\frac{}{\mu^l} \frac{\partial p_c}{\partial s} \nabla s\right] - \nabla \cdot \left[\frac{\rho_l K_{rl} K}{\mu^l} \nabla p\right] = S$	Experimental and model comparison	2D	Water saturation level is highest in the catalyst layer Water saturation level is minimum in micro-porous layer Micro-porous layer serves as a barrier for liquid water and prevents covering up of the interface between gas flow channel and the GDL, thus, increasing the species transport in the porous media
11.	Coppoet al. [75]	Agglomerate	$\frac{\partial s}{\partial t} + \vec{\nabla} \cdot \left(\vec{u}_l s\right) - \vec{\nabla} \cdot \left(D^l_{H_2O} \vec{\nabla} s\right) = S$	Experimental	3D	High temperature increases the reaction rate Higher temperature results in higher membrane conductivity Higher temperature increases the species diffusivity Higher water diffusivity results have been noticed by increasing the temperature in a highly hydrophobic materials Water advection increases at the interface of GDL and gas channel at higher levels
12.	Zhou et al. [83]	Tafel equation	$\frac{dN_{\#,\text{liquid}}(x)}{dx} = \left(\frac{k_c h d}{R_u T_{\#}(x)}\right) \left[\frac{N_{\#,\text{vapor}}(x)}{\sum_i N_{\#,i}(x)} \left(p_{\#}(x) - p_{\#,\text{sat}}(x)\right)\right]$	X	2D	Humidification of anode and cathode inlet is very important Water content on the anode side dominates the membrane performance by delivery the protons to the cathode side Liquid water injection at anode improves cell performance while injection at cathode hinders the effective water removal Pressure loss in PEMs is one of the major parameters affecting the overall performance of cell High inlet humidity at cathode decreases the overall system performance by increasing the pumping power
13.	Berning and Djilali [86]	Tafel equation	Schlögl equation for liquid water through membrane	Experimental	3D	Distribution of three dimensional flow velocities, species concentration, mass transfer rates, electric current and temperature were illustrated

Table 3 (*Continued*)

	Author	Chemical kinetics	Saturation equation	Model validation	Geometry	Major conclusions
14.	Hu et al. [22,87]	Butler–Volmer	$s = \frac{V_W}{V_p}$	Experimental	3D	Interdigitated flow fields enhance the reaction rates by providing better flow through GDL as compared to other flow field distributions Water saturation levels are low with interdigitated flow fields The humidification of inlet species is more significant when utilizing interdigitated flow fields as compared to conventional flow fields
15.	Wang et al. [66]	X	$s = \frac{C^{H_2O} - C_{sat}}{(\rho_l / M_{H_2O}) - C_{sat}}$	Experimental	2D, 3D	Liquid water buildup is faster near inlet region under full humidification inlet conditions Liquid saturation level upto 20% was observed near inlet It was observed that water was trapped at geometric changes (bend etc.)

due to the electro-chemical reactions, the ohmic losses and the heat of evaporation and/or condensation were explicitly considered in this model. The calculation domain consisted of two porous layers of the cathode of PEM fuel cell. The geometry considered in this model was interdigitated flow field with two regions of the porous media distinguished according to the position, i.e., the area under the inlet or the area under the current collector. Finite element technique was employed to the solution domain considering the liquid flow force due to the imbalance of the liquid water pressure and the gaseous pressure. The correlation provided by Leverett [68] was employed to quantify the water saturation effects in the porous media.

Senn and Poulikakos [45] have also presented a 2D model of PEM fuel cell that accounted for multi-component species diffusion, formation of liquid water, heat transfer and electronic current. All the governing equations in this model were non-dimensional and FVM was employed to solve the equations. The main focus of the work was to study the effects of varying the channel, current collector and GDL dimensions. The catalyst layer was assumed to be very thin and treated as a boundary condition for the electro-chemical reactions and the heat source. The distinguished feature of this work was the introduction of a performance variable based on the average current density to measure the effects of mass transfer, water saturation and heat transfer.

A two-phase flow model has also been presented by You and Liu [69,70] for the cathode of PEM fuel cell. The concept of multi-phase mixture model coupled for the porous media and the gas channel was implemented to study the saturation effects. The model presented by Wang and Chen [71] was extended to incorporate detailed effects of levels of multi-phase mixtures instead of separate phases (i.e., two fluid model) including non-zero interfacial areas. The multi-phase model used in this work is derived as given by Wang and Chen [71] and Abriola and Pinder [72]. This model was limited to 2D and the cathode of a PEM fuel cell and explicit results were obtained for the current density affected by different saturation levels along with inlet air humidification.

Siegel et al. [73] also carried out comprehensive modeling of a 2D PEM fuel cell including water transport within the porous media by the capillary pressure. The rate equation for electro-chemical reactions was adapted to the agglomerate structure of the catalyst layer. Major focus of this article was to study the effects of different factors affecting the PEM performance, e.g., geometry, porosity, and polymer properties, etc. The physical properties used in this model were derived by direct measurement from a base case fuel cell experimental model. The results obtained from these simulations were used to study the effect of liquid water on reaction rate and local decrease in the porosity of the catalyst layer and GDL.

Yu et al. [74] presented a 3D model with interdigitated flow field for a PEM fuel cell. In this work two-phase flow and transport mechanism was developed to study the performance of a cell under different operational parameters. A detailed physical insight was provided for the velocity, the species concentration, the water content and concentration, and the current density distribution. All the model equations were discretized using finite volume technique and simulated using commercial CFD software. Coppo et al. [75] also developed a CFD model that incorporates all the major phenomena in PEM fuel cell, i.e., three-phase flow (the third phase refers to the dissolved phase), proton and species transport etc. and agglomerate model was employed to determine the reaction kinetics. The pivot of this work was to evaluate the temperature dependence of all the physical properties used in general PEM models. Moreover, a novel model was also incorporated to describe the liquid water from the porous media surface by advection of water droplets due to the gas streams in the gas channel. All the simulations were performed at different temperature levels and experimentally verified for the accuracy of this approach.

Another complete 2D PEM fuel cell model with two-phase flow was presented by You and Liu [70]. This model was a continuation of earlier models presented by same authors [69,76]. A coupled flow, species, electrical potential and current density was solved in the flow channels, GDLs, catalyst layer and the membrane. The coupling of governing equations on both the cathode and the anode

sides including the membrane provided a much deeper insight of the various parameters and water content. To obtain a converged solution, the authors first assumed the overpotential at the catalyst/membrane interface and calculated the local current density which in turn was used to simulate the net water flux across the boundary and the protonic current. Finally the oxygen and the calculated water flux were used as the boundary condition for the working domain. All the coupled equations were solved iteratively and the average current density was measured by averaging the local current densities along the flow path. Acosta et al. [77] also presented a 2D, non-isothermal, two-phase model for PEM fuel cells with both conventional and interdigitated flow field designs. A continuum approach was utilized to simulate gas and liquid water with extended Darcy's law. The physical properties used in the model, e.g., wettability, permeability and porosity etc., were determined experimentally. For the measurements of the saturation content in the porous media, a method based on mercury intrusion porosimetry was used to quantify the capillary pressure. This model was also limited to the cathode side only and the continuum approach was used to solve the coupled governing equations. All the governing equations were solved iteratively using an in-house code called MUFTE_UG which is based on the concepts and algorithms presented by Helmig [78] or Class [79]. For simulation of water saturation, the Eulerian approach was used where discontinuities in pressure between the two fluid interface was balanced by employing the capillary pressure effects that exist in the porous media.

Meng [80] presented a multi-dimensional two-phase model including a micro-porous layer sandwiched between the catalyst layer and the GDL. A micro-porous layer has been found to reduce the water saturation levels thus enhancing the oxygen transport to the reaction sites and the efficiency [81]. This model has enhanced techniques employed to properly incorporate the interfacial liquid water transport phenomena between the different porous media. Furthermore, the effects of the current collector and the gas flow channel on the saturation of the porous media have also been explicitly studied. The results of this model were verified with high-resolution neutron imaging data [82] and other numerical data. Zhou et al. [83] has also presented a multi-phase and -component 2D model of a PEM fuel cell with pressure and phase change effects to further understand the influence of the inlet humidification and pressure. One of the major assumptions in this model was that liquid water was assumed to exist in form of small droplets with no volume. Berning and Djilali [84–86] also carried out series of 3D work to study the effects of temperature and water management on the performance of fuel cells. In their work, a single fuel cell was divided into one main and three sub-domains. All the domains were coupled through adjustment of appropriate boundary conditions. Similarly, Hu et al. [22,87] also developed and analyzed a two-phase PEM model considering species transport in both anode and cathode sides. A special consideration was given to the impact of ribs on the species transport and SIMPLE algorithm with fourth order Runge–Kutta method was used in their model.

4.2. Experimental analysis of water transport

Additionally, many authors have experimentally studied water transport for specific components of PEM fuel cells, i.e., the catalyst layer, the membrane and the GDL that are of paramount importance because individual component has different behavior under different saturation and water content levels. A brief description of such methods is presented here with briefly stating the findings of the studies.

There are two types of water transport in the membrane of a PEM fuel cells, the electro-osmotic drag and the back diffusion [88]. For complete understanding and accurate modeling of membrane materials it is very essential to accurately estimate the electro-osmotic and back diffusion coefficient of the membrane material. Yan et al. [89] reported a value of 1.5–2.6 for drag coefficient for Nafion^{TM} 117 for different inlet humidification conditions. Similarly Ge et al. [90] determined that varying the thickness of the membrane of the PEM fuel cell has significant effect on the water transport through the membrane and hydrophobicity of the membrane material also alters the absorption and desorption of water at the membrane/catalyst interface thus impacting the overall water transport through the membrane material.

The flooding of the GDL is one of the most investigated phenomena in numerical work but Yamada et al. [91] performed experimental analysis for the extent of water flooding of the cathode GDL with switching interdigitated and conventional flow field designs to measure pressure drop and concluded that water flooding is a direct function of the wetting properties of the catalyst layer and the GDL. Additionally Benziger et al. [92] measured the resistance to the flow of water through the GDL by applying hydrostatic pressure across the GDL and the effects of pressure on the water transport through the voids were analyzed in detail. It was concluded that water flowed through only 1% of the void volume in the GDL. Lin and Nguyen [93] also employed pressure drop calculations to measure the effect of GDL thickness and hydrophobicity on flooding levels. An optimum condition was suggested for both water flooding levels and the species transport through the porous GDL because the hydrophobic pores support the gaseous transport while the hydrophilicity aided the liquid water transport. It was also noticed that employing micro-porous layer (MPL) in-between the catalyst layer and GDL reduced the water flooding which makes it possible to use thinner GDLs for same operation performance level of PEM fuel cell. Litster et al. [94] developed a novel approach to visually study the water flooding levels in the porous GDL by using fluorescence microscopy technique. The movement of water was monitored by following the light emitting dye with a microscope fitted with CCD camera. It was shown that liquid water is transported by fingering and channeling similar to the blotting paper effect.

In many CFD analysis of PEM fuel cells, the flooding of the gas channels is usually ignored keeping in view the fact that liquid portion makes up only minute fraction of the total volume of the gas channel. However, it is very desirable for liquid water in gas channels to be removed because of two adverse effects that can severely degrade the effective operation of PEM fuel cells, i.e., flooding in channels cause a liquid film to cover the GDL surface and hinders in optimum transport of gaseous species inside GDL. And, removal of liquid water at shutdown may not be performed adequately [88]. Kumbur et al. [95] have experimentally investigated the droplet behavior and instability in rectangular PEM fuel cell channels because the physics of detachment size and behavior of water droplets plays an effective role in the liquid water removal from a surface. The findings of this work indicated a strong relation between contact angles (wettability) and the departure diameter on each other along with the surface roughness of the GDL and the characteristics of the fluid flow through the channel. Zhang et al. [60] have also performed similar investigations but mainly focused on the water accumulations at the geometric corners of the flow field at low flow rates.

4.3. Case study of liquid water simulation in a cathode of PEM fuel cell

A two dimensional model of a cathode of PEM fuel cell has been simulated to study the effect of liquid water on the performance in terms of current density and voltage. The reason of selecting the cathode side only is based on the fact that the oxygen reduction reaction (ORR) is the rate limiting reaction in PEM fuel cell electro-chemistry [65]. The salient features of this work are that

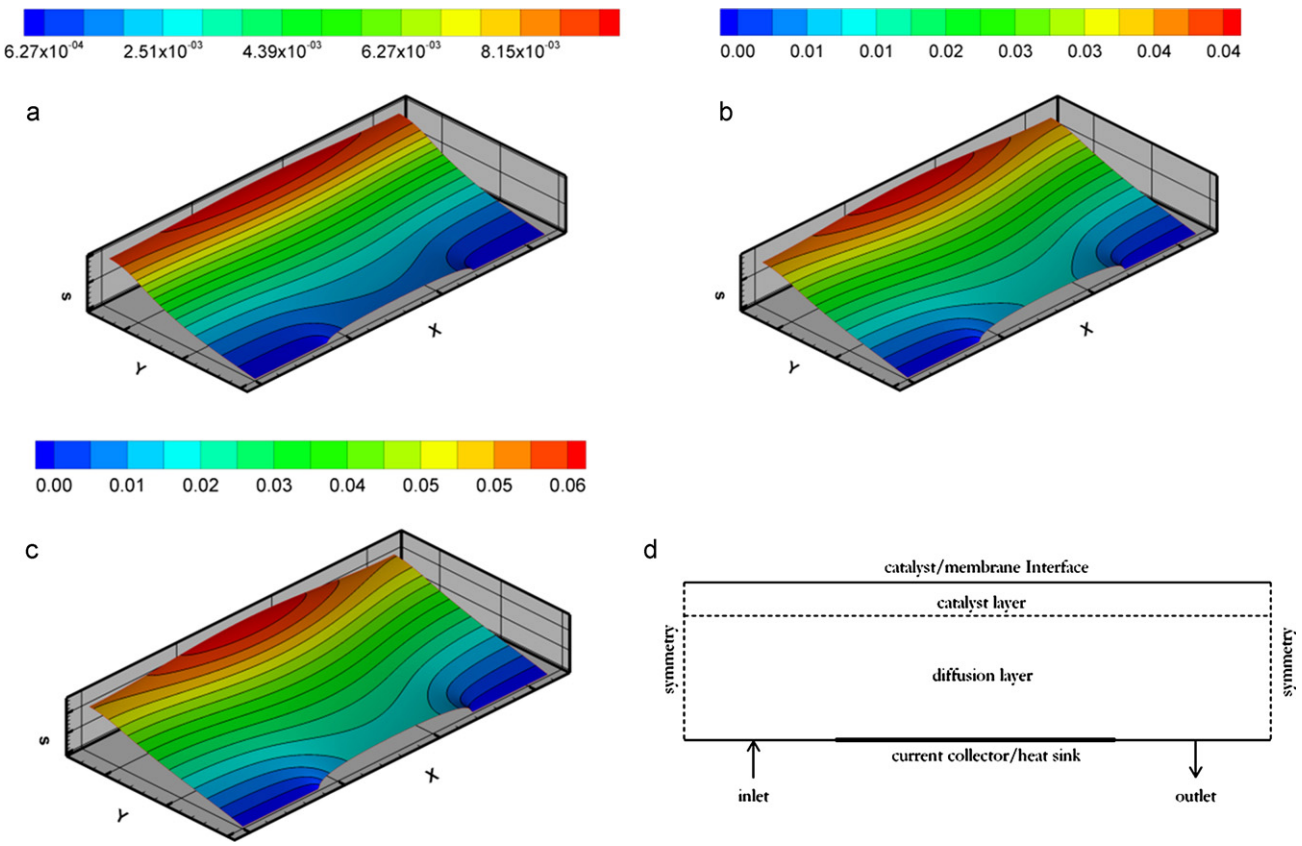

Fig. 3. Contours of water saturation at different current loads; (a) 0.2 A cm^{-2}, (b) 0.5 A cm^{-2}, (c) 0.8 A cm^{-2} (d) the calculation domain.

agglomerate catalyst model was used to predict the reaction rate and the effect of Knudsen diffusion was also included alongside multi-component diffusion of gaseous species as given in Eqs. (8) and (9). To include the effect of temperature, LTNE approach was utilized because it has been previously established [46,48] that fluid temperature is lower than predicted by one equation model because of higher thermal conductivity of the solid structure of the media. All the simulations were performed on Fluent® with 3rd order of spatial dicretization of the domain. In this case, both the inlet and the out of the domain were simulated as infinite sink for liquid water, i.e., zero saturation value at the both the boundaries of the working domain (Fig. 3d).

The simulated results of the water saturation for three load levels i.e., 0.2, 0.5 and 0.8 (A cm^{-2}) are presented in Fig. 3(a, b, and c). In all cases it can be seen that despite of zero water saturation values at the inlet and outlet, the catalyst layer is the most affected part having higher levels of water saturation as compared to GDL that can cause significant loss in efficiency of overall process by making reaction sites unavailable for the reactions. Also, it can be seen that by increasing the current density or load the saturation level also increases suggesting higher reaction rates and water production according to Eq. (2). Other sources that contribute to the overall generation of water are condensation of water vapors and the electro-osmotic drag that can move one to five water molecules from anode to cathode per ion transfer [96]. Although, operation at low loads inherently safe guards the cathode from water flooding but at such conditions a significant loss in protonic conductivity was also observed as compared to high load operation of PEM fuel cell.

To validate the model, the results of this case study were compared to those produced by Sun et al. [97] in which the agglomerate model for electro-chemical reactions was developed to study the influence of the structural parameters on the catalyst layer. As seen in Fig. 4 that both the predictions almost coincide at low current densities but as the current density is increased a gradual deviation is observed between the two cases where the model presented by Sun et al. over-predicts the current density. This deviation between the two cases can be attributed to the effects of water saturation because the model presented by Sun et al. was single phase only i.e., no liquid water was assumed to exist in the computational domain. So, it can be concluded that one of the effects of liquid water inside calculation domain is to limit the reaction kinetics by effectively covering the reaction sites and blocking the path of the reactant gaseous flow.

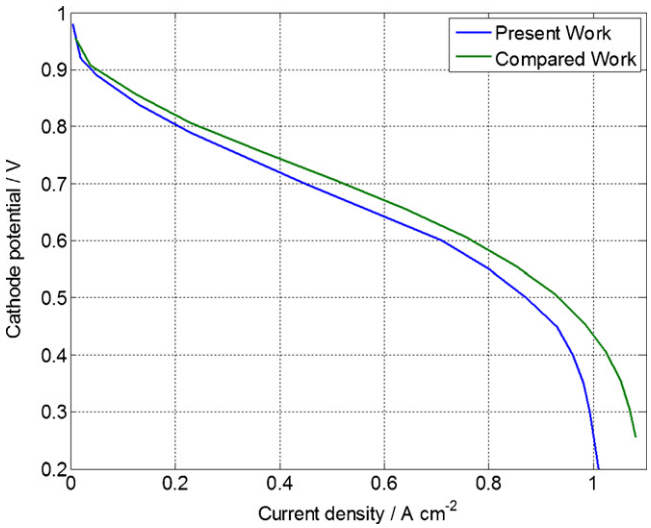

Fig. 4. Comparison of single and two-phase models for PEM fuel cells.

4.4. Two-phase model discrepancies

The list of two-phase models for PEM fuel cells can continue to an infinite number. Many authors, as reviewed before, have produced novel models and validated their results against previously established or experimental work. With increase in the computational power, the numerical modeling of the PEM fuel cells has outpaced experimental work. However, experimental work is still considered the ultimate test for all CFD models and for thorough validation it is necessary that a comparison check should be made between theoretical (CFD) and experimental findings. Keeping this in view, Mench [16] has recently compared the CFD work with high-resolution neutron and X-ray imaging results of liquid water distribution by Turhan et al. [98], Weber and Hickner [99] and Hartnig et al. [100] and found out that various assumptions and theories about liquid water distribution are actually quite misleading under normal operating conditions and development of new models was highly urged. The miss-match of experimental and theoretical findings can be attributed to the reasons discussed below (for detailed discussion the readers is referred to [16], this section only summarizes the latest findings in the same reference).

4.4.1. Large liquid water accumulation at CL/MPL interface

Two phenomena have been pointed out by Mench [16] that result in accumulation of liquid water in large quantities at the CL/MPL interface;

i) Due to the surface roughness of mating catalyst layer and MPL, there is always a chance that large voids regions are left behind even at high commercial scale compactness.
ii) Cracks found at the stated interface are highly probable. As reported by Mench [16], cracks of 20 μm wide may run through MPL and CL and constitute total of 8% of the surface areas.

In CFD modeling the above two anomalies are generally neglected and a perfect CL/MPL interface is assumed. Recent X-ray images [100] have shown a large quantity of water accumulation at the interface and sometimes they represent 5–20% of the total liquid water. Furthermore, the presence of large scale cracks alters the flow pattern of liquid water by providing large flows through these cracks.

4.4.2. Applicability of Leverett function for liquid water distribution

Not all, but many two-phase models proposed for water management in PEM fuel cells utilize the Leverett function that gives dominance to capillary flow in the porous media, given as [101];

$$J(s) = \frac{P_c}{\sigma}\sqrt{\frac{K}{\varepsilon}} \tag{10}$$

where P_c, σ, ε and K represent the capillary pressure, interfacial tension between phases, porosity and the absolute permeability of the medium, respectively. However, the proposed Leverett function (also called J-function) was initially proposed for flow of water through soil, whereas, the porous media used for PEM fuel cell construction is highly compact and anisotropic in nature. Kumbur et al. [102] has shown that significant deviation in direct measurement of water quantity as compared to the proposed distribution by the Leverett function. So, it is very urgent that new and well descriptive governing equations are developed for water flow in PEM fuel cell porous media. Recently, Kumbur et al. has proposed new relationships for governing the capillary flow in PEM porous media [103–105], based on direct measurement by experimental techniques.

4.4.3. Bruggeman's relation

Usually the effect of saturation in the porous media is approximated by Bruggeman's relation that only restricts the flow of species in terms of reduced porosity, as;

$$D_{\text{eff}} = D_i \times \left[\varepsilon^{\tau}(1-s)\right] \tag{11}$$

According to Eq. (11), the only effect by the presence of liquid water is to reduce diffusivity of the gaseous species by reducing the void volume in porous media. However, as noted by Mench [16], this relation ignores the effect of blocking of pathways for gaseous flow through porous media that can significantly affect the fuel cell performance.

4.4.4. Other discrepancies in two-phase models

Apart from the previously explained ignorance reigning the two-phase models, few more considerations need to be taken into account for vivid description and picture of saturation in PEM fuel cells, as outlined here;

i) The inter-phase change between water humidified gaseous species and liquid water is usually modeled as [8,23];

$$\dot{m}_{\text{Phase}} = \begin{cases} k_{\text{con}}(1-s)X_{H_2O}\dfrac{P_{H_2O} - P^{\text{sat}}_{H_2O}}{RT_f} \\ k_{\text{evp}}\left(\dfrac{\rho_w}{M_{H_2O}}\right)\left(P_{H_2O} - P^{\text{sat}}_{H_2O}\right) \end{cases} \tag{12}$$

The evaporation/condensation process in PEM fuel cells is governed by the saturation pressure of the water vapor and the temperature. The validity of this process is still a question mark as it has not been experimentally verified and experimental works suggest that even fractional difference in temperature can have significant deviation from the simulated results by Eq. (12) [16].
ii) Modeling of liquid water distribution, usually a porous jump condition is assumed at the interfaces of components because of the difference in porosity and radius of pores in two adjacent materials to account for the continuity. These assumptions predict that GDL has more capacity to store liquid water as compared to MPL because of its higher porosity, but, experimental results show the other way, i.e., GDL represents low accumulation region for liquid water [16].

As discussed above, despite of active model developments for PEM fuel cells and understanding the water management issue, many inter-related phenomena still need to be accounted and a vigorous and robust approach is required that can encircle all the PEM fuel cell issues and produce efficient and stable results that can help in commercialization and help PEM fuel cells to compete with highly developed conventional counterparts that have taken centuries to grow and groom.

5. Meso-scale models for the cathode

The electrodes of a PEM fuel cell are volumetric and are composed of catalyst layer and GDL. One of the key components of PEM fuel cell is the catalyst layer where electro-chemical reactions take place. The catalyst layer is often made of porous mixture of carbon supported platinum particles (Pt|C), ion and electron conducting material (Nafion), and also provides the transport of reactant gaseous species to the reaction sites. Each electrode in PEM fuel cells is separated by an ion conducting electrolyte that is usually 20–100 μm thick [106]. The Pt|C particles have the typical dimensions of 100 nm and are thoroughly distributed in the catalyst layer. Furthermore, Pt|C particles are covered with the same

ionic conducting material ($\sim 10^{-7}$ m thick [107]) as used in electrolyte preparation to insure three-phase contact. Additionally, for even distribution of the gaseous species and the electron conduction from/to the catalyst layer, a GDL is incorporated to a thickness of mm. On component and system scale, the dimensions are ranged between 10 and 100 cm and more [108]. In order to encompass all the length scales in PEM fuel cells, a multi-scale model needs to be developed that has much shorter range (beyond continuum approximation) than current CFD scales that are mostly based on Navier–Stokes. For categorization of the fluid flow regime, the most commonly tool used is the Knudsen number defined as;

$$k_n = \frac{\lambda}{l} \tag{13}$$

where λ is the mean free path of the molecules, and l represents the characteristic flow dimension. The selection of the characteristic dimension depends on the length scales of the gradients of pressure, density, velocity and temperature. The Knudsen number is useful for determining whether statistical mechanics or the continuum mechanics formulation of fluid dynamics should be valid: if the Knudsen number is near or greater than one, the mean free path of a molecule is comparable to or larger than the length scale of the problem, and the continuum assumption of fluid mechanics is no longer a good approximation. In recent years, for PEM fuel cell multi-scale modeling many authors have opted the Lattice Boltzmann (LB) method which is applicable over the whole range of Knudsen number, including the continuum regime. The LB method provides a better alternative to conventional CFD analysis of fluid flow for deeper insight.

5.1. Lattice Boltzmann method for fluid flows

In recent years, Lattice Boltzmann (LB) method has emerged as an alternative simulation tool for predicting fluid flows and has been found very successful for interfacial dynamics and complex boundaries. Lattice Boltzmann method is based on microscopic models and mesoscopic kinetic equations, unlike conventional numerical methods in which macroscopic equations are discretized over the spatial domain [109]. The underlying theory of the Lattice Boltzmann method is to develop simplified kinetic models capturing key features of micro- or mesoscopic physics so that the desired macroscopic equations are satisfied since macroscopic fluid flow is a collection of many microscopic particles in the system [109,110]. Here, the LB method is briefly presented for basic know-how, for detailed understanding one can refer to Succi [111], Chen and Doolen [109], Sukop and Throne [112], Park et al. [113], and Spaid and Phelan [114].

The Lattice Boltzmann method is a mesoscopic method that is considered in-between the continuum based technique and the molecular dynamics technique which handles individual particles in the flow field. In this method, a large group of molecules are assumed to move about a lattice and collide with each other. At each lattice point, the particles translate at discrete directions and all particles in one direction are grouped together. Generally LB method can be divided into two sequential steps as (i) streaming and (ii) collision. The streaming process describes the movement of a particles to adjacent lattice point in the direction of travel while keeping mass and momentum as conserved quantities. The intra collision of particles is defined by the collision step [115]. The general governing equation for the LB method is given as [109];

$$n_i(\mathbf{x}+\mathbf{e}_i\Delta x,\ t+\Delta t) = n_i(\mathbf{x}, t) + \Omega_i(n(\mathbf{x}, t)) \quad i = 0,\ 1,\ \ldots,\ M \tag{14}$$

The Eq. (14) is itself quite cumbersome to solve because of an infinite sets of particles moving along different directions and collisions occurring with respect to the scattering rule. A modification is generally enforced to limit only one particle moving in certain direction with a certain velocity. This simplification is termed as the exclusion principle and reduces tracking of particles to a finite and manageable number for a given time step [109]. For scattering step, which is non-linear in nature, Higuera and Jiménez [116] proposed to assume the distribution close to equilibrium state to avoid non-linearlization. In Eq. (14), n_i is a real variable representing the mass per unit volume of the particle translating with a speed i, while, $\mathbf{e}_i$ is the direction vector and M represents the total number of lattice points in consideration. For 2D geometries M ranges from 4 to 9, whereas, for 3D cases the total number of lattice points can be either 15, 17 or 19.

Since 1992, a considerable attention has been paid to use LB methods for different technologies. According to the data collected by Sukop and Throne [112], a variety of fields have adopted this technique with physics and mathematics being the main bearers. However, only a few papers with LB method and PEM fuel cells as title or keywords have been produced to date. Here a review of these is presented that are specifically focused on PEM fuel cells.

Generally GDL is treated as homogeneous and isotropic porous material without considering the manufacturing details of the preparing material. Bundles of carbon fibers are used to prepare the carbon papers that are stacked together to form the GDL. Due to the structural alignment of carbon fibers there is strong dependency of physical properties to spatial directions, i.e., in-plane (parallel to surface) and through-plane (perpendicular to surface). As described in [115], GDL can be aptly assumed to consist of randomly arranged cylinders with diameter (7–12 μm) being very small as compared to their length. So, due to inherent alignment formed during making of carbon papers for PEM fuel cells there is a preferential fiber direction. Van Doormaal and Pharoah [115] have applied LB method to determine the porosity, permeability, flow direction and fiber directions to have a deeper insight of GDL. The geometry for this study was generated using the modified Monte Carlo technique by Himilton [117]. The alignment of fibers was varied from 0 to 90°, i.e., from parallel to perpendicular directions and numbers of cases were simulated for all directions with porosity ranging from 0.6 to 0.81. The proposed relation between porosity and the permeability of the GDL by the authors is given as;

$$K = \begin{cases} 0.26\dfrac{\varepsilon^{3.6}}{1-\varepsilon}r^2 & \text{in-plane} \\ 0.28\dfrac{\varepsilon^{4.3}}{1-\varepsilon}r^2 & \text{through-plane} \end{cases} \tag{15}$$

where r is the fiber radius and predictions were found to be within 95% of the prediction by Carmen–Kozeny equation [118].

Park and Li [113,119] have also performed LB simulations for the in-homogeneous GDL of a PEM fuel cell with considering multi-phase flow via two different LB formulations. The simulation domain for this study was 400 μm^2 consisting of voids and solid obstacles represented by the fiber material. It was demonstrated that flow squeezed at narrow paths in-between the fibers causing pressure drop and increase in velocity. Additionally, it was noted that large flow blockages can be caused by even small obstacles due to their inherent orientation and fibers in parallel to the main flow directions had no significant effect on flow resistance implying that the permeability is not only a function of the porosity of the GDL material but it is greatly affected by the orientation of the fibers also. To include the effect of liquid water, the inter-particle interaction model was also used as LB methods are capable of providing robust predictions of the interfaces between two or more phases [119]. One of the findings by the authors was that some of the liquid water moving along the flow direction was captured in the porous media and it can be concluded that the captured water can cause either blocking of the porous path or covering of reaction sites if it is in the catalyst layer. Similarly it was also predicted that LB method is far superior to conventional CFD techniques

to portray unsteady liquid water accumulation/removal process. Karimi and Li [120] carried out numerical calculations for a single pore of the membrane material to investigate the electro-osmotic flow through Poisson–Boltzmann and Navier–Stokes equations, and predicted that the pore dimensions have significant impact on the drag coefficient for water transport. Similar work was carried out on microstructure of the membrane material by Okada et al. [121] to demonstrate the dependence of the ion mobility on the microstructure of the membrane material.

6. Microscopic models for the catalyst layers

It has been already stated in the previous sections that the physio-chemical features of the catalyst layer is one of the performance limiter in PEM fuel cells. The catalytic activity in PEM fuel cells is dependent on the catalyst particle size, shape, distribution, gaseous access to the reaction sites, ionic and electronic conductivity and thermal distribution. Catalyst material, processing and catalytic reactions are all inter-related disciplines and a good optimum design can only ensure high performance catalyst layer [122].

Liu [122] has developed top–down and bottom–up approaches in analysis of the catalyst materials. In top–down approach, a multi-scale analysis approach is used to segregate the catalyst material into individual technology components signifying the interaction of each to the overall performance, while the bottom–up approach helps in developing and improving the catalyst design and stability. Although, with advances in modern science and technology, higher degree of understanding has been attained for the catalyst materials and performance, but still, it is treated as a black box in most of the modeling techniques. A need is felt here to study the catalyst layer at particle or pore-size levels.

6.1. Catalyst layer modeling at particle- and pore-size level

The catalyst layer in PEM fuel cells forms the backbone of the unit cells. Apart from the design considerations for other components, the optimization of the catalyst material and its distribution inside the layer is very essential for high performance and utilization. Recently it has been developed that manipulating the catalyst structures can significantly enhance its performance and for solid catalyst particles as in PEM fuel cells, the decrease in particle size helps in significant performance upgrade and increasing the catalyst size can cause a rapid decline in performance [122]. Since Pt is an expensive metal, the control of catalyst design is very eminent for commercial competition of PEM fuel cells with other available energy production devices.

Lee and Cho [123] determined, through chemical quantum calculations, that the arrangement of individual Pt particle can lead to the optimization of catalyst utility and performance. Configurations of 611 Pt atoms with size of 3.1 nm have been found to be the most suitable. However, in PEM fuel cells, not only the size and configuration are important but transport of ions, electrons and reactants to the catalytic sites is also very essential. In PEM fuel cells, coating of larger carbon particles with nano-sized Pt particles submerged in electrolyte material has been termed as one of the most effective catalytic distribution patterns for high utilization [39,124]. The parameter used to describe the performance of the catalyst in PEM fuel cells is the effective surface area in PEM fuel cells [125]. Using finer particle size leads to an increased effective surface area per unit volume of the catalyst particle and increasing of the catalyst loading (mass per unit surface area) also results in increased reaction rates [125].

Recently, Siddique and Liu [126] have digitally constructed a 3D model of the catalyst layer at nano-scale using controlled quasi-random algorithms numerically duplicating the experimental fabrication process aiming to quantify porous nanostructure and investigate the mechanism of nano-scale electro-chemical reactions and percolation networks. It was concluded that a threshold percolation exists for species transport through the catalyst structure and also altering the optimum value of the agglomerate number reduces the electro-chemical reactions. Similarly, Lange et al. [127] also performed 3D nano-scale simulations by reconstructing the catalyst layer using a stochastic approach. The focus in this work was to compute effective transport parameters over selected sets of operating conditions for variety of microstructures. Additionally, the effects of water vapor and temperature profiles have been studied in depth. For the validation of the computed results, a detailed comparison has also been performed by experimental results by the same group [128].

6.2. Agglomerate modeling approach

In open literature many mathematical models for the catalyst layer have been proposed from zero to three dimensional models. Among all, the flooded agglomerate model is the most descriptive and predicting model [129]. In this model, the carbon supported Pt particles in form of agglomerate are immersed in a thin film of electrolyte. The catalyst layer consists of a network of interconnected micro- and macro-sized pores through which the gaseous species reach the surface of the agglomerates. There upon, the reactant species diffuse through a thin layer of the electrolyte to reach the reaction site [130]. The agglomerate model has been able to give deeper insight into the physio-electro-chemical phenomena in simulations and modeling of the catalyst layer. However, the consideration of the catalyst layer to be composed of carbon supported Pt with flooded electrolyte film as a continuum medium has made it difficult to analyze the discrete distribution of the catalyst phase in the agglomerate [131].

Yan and Wu [130], Antonio et al. [132] and Bultel et al. [133] have developed various micro-models for the catalyst layers in which mass and ion transfer have been addressed separately by treating the agglomerate and the electrolyte material (Nafion) as discrete and segregated components. The proposed micro-models have been able to provide deeper insight into the detailed mass and ion transfer mechanisms at pore levels, and particle size relation and dependence in the overall performance for the electro-chemical reactions.

The relation between the generation of the current per unit volume as a function of electric and ionic potentials, reactant concentrations and the material properties of the catalyst layer is represented by a modified Butler–Volmer kinetics as [134–136];

$$\nabla \cdot \mathbf{i}_1 = 4FC_{O_2}^{\text{bulk}} \left(\frac{\delta_{\text{film}}}{A_{\text{agg}} D_{O_2,\text{nafion}}} + \frac{1}{kE} \right)^{-1} \tag{16}$$

where δ, A_{agg}, $D_{O_2,\text{nafion}}$, k and E represent the thickness of Nafion covering the agglomerate, agglomerate area, diffusivity of oxygen through electrolyte, reaction rate and the effectiveness factor. Considering the first order reaction kinetics, the analytical expression for the effectiveness factor yielded by applying the mass conservation equation for spherical agglomerate is given as [136];

$$E = \frac{1}{3\phi^2} \left[3\phi \coth(3\phi) - 1 \right] \tag{17}$$

where ϕ is the Theiles modulus for the system and is expresses by [8];

$$\phi = \zeta \sqrt{\frac{k}{D_{O_2,\text{nafion}}}} \tag{18}$$

in which, ζ is the characteristic length of the agglomerate in terms of volume per unit surface area, usually given as $R_{agg}/3$ for spherical structures as used in preparation of catalyst for PEM fuel cells [136].

7. Model verification

Since all numerical studies have been done theoretically by solving a combination of equations backed by empirical or experimental data with a set of assumptions to make it feasible with respect to both time and computational power at hand, it is very important to validate the results obtained. Most of the fuel cells models have been validated against the measured data using the polarization curve or V–I curve. But mere comparison with V–I curve does not ensure complete robustness and accuracy of the predicted results [16]. According to Mench [16], it is not surprising that a good agreement between the model and a simple polarization curve can be achieved but does not necessarily validate the internal distribution of parameters like heat, water, and charge, since underprediction of one parameter may be balanced by over-prediction of other and vice versa. Additionally, fuel cell system performance fluctuates with different electrode assemblies, however, the numerical simulations are not flexible enough to accommodate all details to represent the fluctuations in the performance [16]. Similarly, Pharoah et al. [43] has also reported anomalies in model comparison methods using the V–I curve for different cases while reviewing the material anisotropic effects on the fuel cell performance. It was noted that the V–I curve for both anisotropic and isotropic electronic conductivity were almost identical, however, the internal current distributions varied significantly for different load conditions. For the same load, the maximum current density occurred under the rib area of the fuel cell for the isotropic conditions but since the anisotropy of electrical conductivity makes the conduction much higher in in-plane direction, it was noticed that the maximum shifted to the channel center line in the latter case.

Since fuel cell predictions are dependent on a number of parameters, and most of which have not yet been properly characterized. Usually to match the predictions, one or more parameters are tuned to obtain matched results via single V–I curve. But, proper validation of numerical models can only be achieved by a comparison with detailed and local experimental data and results, but lack of such data prohibits the proper validation. Since fuel cells are relatively infant in age comparatively, there is a tremendous need to develop methods and techniques for real-time data acquisition for validation of numerical models. However, it has been suggested by Pharoah et al. [43], in absence of real-time data, that different V–I curves under various operating conditions should be compared. Although this will not ensure complete validation of the models but operation under different set of conditions will posturize the general trend in the performance response of a fuel cell model.

8. Conclusions

PEM fuel cells represent a promising future for the energy production with low to zero greenhouse gas emissions. Although, many advancements have been made in the recent years in PEM technology both in terms of insight into internal phenomena and development, however, some major issues still need to be addressed before rendering PEM fuel cells for large scale commercialization. Among many, water management is an old time problem that has not been fully understood and characterized. Since PEM fuel cells operate under different load conditions, it is quite difficult to set a fixed parameter for the quantity of water as at higher load conditions removal is deemed necessary to avoid blocking of both reaction sites and pathways for gaseous flow, while in low operation levels less water quantity exhibits a decreased ionic conductivity of the electrolyte. So, it is very eminent that the water management issue has to be resolved in the near future to make PEM fuel cell competent with respect to other fuel cell types and conventional energy sources. With the advances in computational technologies in terms of both speed and efficiency, CFD has become an optimum tool to perform detailed study of PEM fuel cells in all aspects from understanding the internal phenomena to design optimization. A great deal of work has been done since then with a variety of models and results. Initially, most models were limited to 2D and single phase flows. But, with deeper interest in managing the water issue inside PEM, later models developed were extended to two-phase with both 2D and 3D geometries. But still a complete model has not been produced yet basically due to both computational limits and inherent complex phenomena occurring inside PEM fuel cells. The discrepancies in modeling water management issue still needs a deeper insight ranging from development of new formulations to include physical and chemical effects. A test case was also presented to study the effects of water saturation. It was observed that the catalyst layer was the most affected area as maximum water saturation effects were noted there with increasing trends with increase in operating current densities.

Although CFD analysis has provided an overall behavior of PEM fuel cells but complete validation of the results in terms of robustness and capability to predict the transport phenomena still needs to be verified against experimentally established results, as it has been often observed that although the predicted V–I curves have same profiles but internal distribution of parameters like current density, heat and water saturation may vary significantly. Also, PEM fuel cells involve multi-scale parameters and phenomena, e.g., the electro-chemical reactions and the charge transport which are best evaluated at micro- or meso-scale levels, so, the multi-scale approach will further elaborate the secretive picture of the fuel cell operations. Recent developments in application of Lattice Boltzmann method to flow analysis provides the facility to simulate the flows at meso-scale, although, it is computationally expensive to apply to a complete single cell presently, but use of this method to PEM fuel cell technology is pacing up and some researchers have already proven its worth in evaluating physical properties such as permeability with direction dependent profiles when applied to selective and manageable dimensions. Further development in this field can be explored to reveal more insight to PEM fuel cells and establish robust and reliable results.

Acknowledgement

The financial support from the European Research Council (ERC 226238-MMFCs) is gratefully acknowledged.

References

[1] N. Summes, Fuel Cell Technology – Reaching Towards Commercialization, Springer, London, 2006.
[2] B. Sundén, M. Faghri, Transport Phenomena in Fuel Cells, WIT Press, Southampton, 2005.
[3] C. Siegel, J. Energy 33 (2008) 1331–1352.
[4] D. Cheddie, N. Munroe, J. Power Sources 147 (2005) 72–84.
[5] D. Natarajan, T. Van Nguyen, J. Power Sources 115 (1) (2003) 66–80.
[6] H. Li, Y. Tang, Z. Wang, Z. Shi, S. Wu, D. Song, J. Zhang, K. Fatih, H. Wang, Z. Liu, R. Abouatallah, A. Mazza, J. Power Sources 178 (1) (2008) 103–117.
[7] C. Song, Y. Tang, J.L. Zhang, J. Zhang, H. Wang, J. Shen, S. McDermid, J. Li, P. Kozak, Electrochim. Acta 52 (7) (2007) 2552–2561.
[8] M. Khan, Numerical simulation of multi-scale transport processes and reactions in PEM fuel cells using two-phase models, Licentiate Thesis, ISRN LUTMDN/TMHP-09/7066-SE, Lund University, Lund, 2009.
[9] X. Ren, S. Gottesfeld, J. Electrochem. Soc. 148 (1) (2001) A87–A93.

[10] J.T.A. Zawodzinski, C. Derouin, S. Radzinski, R.J. Sherman, V.T. Smith, T.E. Springer, S. Gottesfeld, J. Electrochem. Soc. 140 (4) (1993) 1041–1047.
[11] D.P. Wilkinson, H.H. Voss, K. Prater, J. Power Sources 49 (1–3) (1994) 117–127.
[12] J.S. Yi, J.D. Yang, C. King, AIChE J. 50 (10) (2004) 2594–2603.
[13] A. Biyikoglu, Int. J. Hydrogen Energy 30 (11) (2005) 1181–1212.
[14] C.Y. Wang, Chem. Rev. 104 (2004) 4679–4726.
[15] K. Haraldsson, K. Wipke, J. Power Sources 126 (2004) 88–97.
[16] D. Stolten, in: M.M. Mench (Ed.), Advanced Modeling in Fuel Cell Systems: A Review of Modeling Approaches, Wiley-VCH, Weinheim, 2010.
[17] F. Standaert, K. Hemmes, N. Woudstra, J. Power Sources 63 (2004) 1231–1242.
[18] Q. Wang, D. Song, T. Navessin, S. Holdcroft, Z. Liu, Electrochim. Acta 50 (2–3) (2004) 725–730.
[19] J. Wishart, Z. Dong, M. Secanell, J. Power Sources 161 (2) (2006) 1041–1055.
[20] T.E. Springer, T.A. Zawodzinski, S. Gottesfeld, J. Electrochem. Soc. 138 (1991) 2334–2342.
[21] W. He, J.S. Yi, T.V. Nguyen, AIChE J. 46 (10) (2000) 2053–2064.
[22] M. Hu, A. Gu, M. Wang, X. Zhu, L. Yu, Energy Conv. Mang. 45 (2003) 1861–1882.
[23] J.J. Hwang, J. Power Sources 164 (1) (2007) 174–181.
[24] N. Djilali, P.C. Sui, Int. J. Comput. Fluid Dyn. 22 (1) (2008) 115–133.
[25] C.H. Cheng, K. Malek, P.C. Sui, N. Djilali, Electrochim. Acta 5 (2010) 1588–1597.
[26] W. Goddard, B. Merinov, A. van Duin, T. Jacob, M. Blanco, V. Molinero, S.S. Jang, Y.H. Jang, Mol. Simul. 32 (2006) 251–268.
[27] H. Kanako, T. Takashi, O. Katsuhide, Int. Symp. Adv. Fluid. Inf. 5 (2005) 55–58.
[28] K. Malek, M. Eikerling, Q. Wang, T. Navessin, Z. Liu, J. Phys. Chem. C 111 (36) (2007) 13627–13634.
[29] M. Meiler, M. Schmid, E.P. Hofer, J. Power Sources 176 (2) (2008) 523–528.
[30] P.R. Pathapati, X. Xue, J. Tang, Renewable Energy 30 (1) (2005) 1–22.
[31] T.M. Brown, J. Brouwer, G.S. Sameulsen, F.H. Holcomb, J. King, J. Power Sources 182 (1) (2008) 240–253.
[32] M. Hatti, M. Tioursi, Int. J. Hydrogen Energy 34 (11) (2009) 5015–5021.
[33] V. Rouss, W. Charon, J. Power Sources 175 (1) (2008) 1–17.
[34] Y.-J. Zhang, M.-G. QOuyang, Q.-C. Lu, J.-X. Luo, X.-H. Li, Appl. Thermal Eng. 24 (4) (2004) 501–513.
[35] M. Meiler, D. Andre, M. Schmid, E.P. Hofer, J. Power Sources 190 (1) (2009) 56–63.
[36] X. Xue, J. Tang, A. Smirnova, R. England, N. Sammes, J. Power Sources 133 (2) (2004) 188–204.
[37] E.A. Muller, A.G. Stefanopoulou, J. Fuel Cell Sci. Tech. 3 (2) (2006) 99–110.
[38] G. Vasu, A.K. Tangirala, J. Power Sources 183 (1) (2008) 98–108.
[39] J. Larminie, A. Dicks, Fuel Cell Systems Explained, John Wiley & Sons Ltd., West Sussex, 2003.
[40] H. Meng, J. Power Sources 161 (1) (2006) 466–469.
[41] U. Pasaogullari, P.P. Mukherjee, C.-Y. Wang, K.S. Chen, J. Electrochem. Soc. 154 (8) (2007) B823–B834.
[42] J.H. Nam, M. Kaviany, Int. J. Heat Mass Transfer 46 (24) (2003) 4595–4611.
[43] J.G. Pharoah, K. Karan, W. Sun, J. Power Sources 161 (1) (2006) 214–224.
[44] F. Liu, C.-Y. Wang, Electrochim. Acta 52 (3) (2006) 1409–1416.
[45] S.M. Senn, D. Poulikakos, J. Heat Transfer 127 (2005) 1245–1259.
[46] J.J. Hwang, C. P.Y., Int. J. Heat Mass Transfer 49 (2006) 2315–2327.
[47] C.H. Chao, A.J.J. Hwang, J. Power Sources 160 (2006) 1122–1130.
[48] A.J.J. Hwang, C.H. Chao, C.L. Chang, W.Y. Ho, D.Y. Wang, Int. J. Hydrogen Energy 32 (2007) 405–414.
[49] H. Ju, H. Meng, C.-Y. Wang, Int. J. Heat Mass Transfer 48 (2005) 1303–1315.
[50] M.F.L. Johnson, W.E. Stewart, J. Catalysis 4 (1965) 248–252.
[51] K. Malek, M.-O. Coppens, J. Chem. Phys. 119 (5) (2003) 2801–2811.
[52] J. Yuan, X. Lv, B. Sundén, D. Yue, Int. J. Hydrogen Energy 32 (2007) 3887–3898.
[53] D. Mu, Z.-S. Liu, C. Huang, N. Djilali, Microfluid. Nanofluid. 4 (3) (2008) 257–260.
[54] ANSYS® Fluent® Software, http://www.fluent.com.
[55] COMSOL Multiphysics®, http://www.comsol.com.
[56] STAR-CD®, http://www.cd-adapco.com/products/STAR-CD/index.html.
[57] CFD-ACE+®, http://www.esi-group.com.
[58] K.H. Choi, D.H. Peck, C.S. Kim, T.H. Shin, T.H. Lee, J. Power Sources 86 (2000) 197–201.
[59] X.G. Yang, F.Y. Zhang, A.L. Lubawy, C.Y. Wang, Electrochem. Solid State Ltrs. 7 (11) (2004) A408–A411.
[60] F.Y. Zhang, X.G. Yang, C.Y. Wang, J. Electrochem. Soc. 153 (2) (2006) A225–A232.
[61] U. Pasaogullari, C.Y. Wang, J. Electrochem. Soc. 151 (3) (2004) A399–A406.
[62] Z.H. Wang, C.Y. Wang, K.S. Chen, J. Power Sources 94 (2001) 40–50.
[63] R. Borup, J. Meyers, B. Pivovar, Y.S. Kim, R. Mukundan, N. Garland, D. Myers, M. Wilson, F. Garzon, D. Wood, P. Zelenay, K. More, K. Stroh, T. Zawodzinski, J. Boncella, J.E. McGrath, M. Inaba, K. Miyatake, M. Hori, K. Ota, Z. Ogumi, S. Miyata, A. Nishikata, Z. Siroma, Y. Uchimoto, K. Yasuda, K.-i. Kimijima, N. Iwashita, Chem. Rev. 107 (10) (2007) 3904–3951.
[64] G. He, Y. Yamazaki, A. Abudula, J. Power Sources 194 (1) (2009) 190–198.
[65] J. Yuan, B. Sundén, Electrochim. Acta 50 (2004) 677–683.
[66] Y. Wang, S. Basu, C.Y. Wang, J. Power Sources 179 (2008) 603–617.
[67] A.D. Le, B. Zhou, J. Power Sources 182 (1) (2008) 197–222.
[68] M.C. Leverett, Pet. Trans., AIME (Am. Inst. Min. Metall. Eng.) 142 (1941) 152–169.
[69] L. You, H. Liu, Int. J. Heat Mass Transfer 45 (2002) 2277–2287.
[70] L. You, H. Liu, J. Power Sources 155 (2) (2006) 219–230.
[71] C.Y. Wang, P. Cheng, Int. J. Heat Mass Transfer 39 (17) (1996) 3607–3618.
[72] L.M. Abriola, G.F. Pinder, Water Resour. Res. 21 (1985) 11–26.
[73] N.P. Siegel, M.W. Ellis, D.J. Nelson, M.R.v. Spakovsky, J. Power Sources 128 (2004) 173–184.
[74] L.J. Yu, G.P. Ren, M.J. Qin, X.M. Jiang, Renewable Energy 34 (3) (2009) 530–543.
[75] M. Coppo, N.P. Siegel, M.R. von Spakovsky, J. Power Sources 159 (2006) 560–569.
[76] L. You, H.T. Liu, Int. J. Hydrogen Energy 25 (2001) 991–999.
[77] M. Acosta, C. Merten, G. Eigenberger, H. Class, R. Helmig, B. Thoben, H. Müller-Steinhagen, J. Power Sources 159 (2) (2006) 1123–1141.
[78] R. Helmig, Multiphase Flow and Transport Processes in the Subsurface – A Contribution to the Modeling of Hydrosystems, Springer Verlag, 1997.
[79] H. Class, R. Helmig, P. Bastian, Adv. Water Resour. 25 (2002) 533–550.
[80] H. Meng, Int. J. Hydrogen Energy 34 (2009) 5488–5497.
[81] J.H. Nam, M. Kaviany, Int. J. Heat Mass Transfer 46 (2003) 4595–4611.
[82] M.A. Hickner, N.P. Siegel, K.S. Chen, D.S. Hussey, D.L. Jacobson, M. Arif, J. Electrochem. Soc. 155 (2008) B427–B434.
[83] B. Zhou, W. Huang, Y. Zong, A. Sobiesiak, J. Power Sources 155 (2) (2006) 190–202.
[84] T. Berning, D.M. Lu, N. Djilali, J. Power Sources 106 (2002) 284–294.
[85] T. Berning, N. Djilali, J. Electrochem. Soc. 150 (2003) A1589–A1599.
[86] T. Berning, N. Djilali, J. Power Sources 124 (2003) 440–452.
[87] M. Hu, X. Zhu, M. Wang, A. Gu, L. Yu, Energy Conv. Mang. 45 (11–12) (2004) 1883–1916.
[88] S.G. Kandlikar, Heat Transfer Eng. 29 (2008) 575–587.
[89] Q. Yan, H. Toghiani, J. Wu, J. Power Sources 158 (2006) 316–325.
[90] S. Ge, X. Li, B. Yi, I.-M. Hsing, J. Electrochem. Soc. 6 (2005) A1149–A1157.
[91] H. Yamada, T. Hatanaka, H. Murata, Y. Morimoto, J. Electrochem. Soc. 159 (2006) A1748–A1754.
[92] J. Benziger, J. Nehlsen, D. Blackwell, T. Brennan, J. Itescu, J. Membr. Sci. 261 (2005) 98–108.
[93] G. Lin, T.V. Nguyen, J. Electrochem. Soc. 152 (2005) A1942–A1948.
[94] S. Litster, D. Sinton, N. Djilali, J. Power Sources 154 (2006) 95–105.
[95] E.C. Kumbur, K.V. Sharp, M.M. Mench, J. Power Sources 161 (2006) 333–345.
[96] A. Thomas, J. Zawodzinski, C. Derouin, S. Radzinski, R.J. Sherman, V.T. Smith, T.E. Springer, S. Gottesfeld, J. Electrochem. Soc. 140 (4) (1993) 1041–1047.
[97] W. Sun, B.A. Peppley, K. Karan, Electrochim. Acta 50 (16–17) (2005) 3359–3374.
[98] A. Turhan, S. Kim, M. Hatzell, M.M. Mench, Electrochim. Acta 55 (8) (2010) 2734–2745.
[99] A.Z. Weber, M.A. Hickner, Electrochim. Acta 53 (26) (2008) 7668–7674.
[100] C. Hartnig, I. Manke, R. Kuhn, N. Kardjilov, J. Banhart, W. Lehnert, Appl. Phys. Lett. 92 (13) (2008) 134106.
[101] http://jgmaas.com/scores/facts.html.
[102] E.C. Kumbur, K.V. Sharp, M.M. Mench, J. Power Sources 168 (2) (2007) 356–368.
[103] E.C. Kumbur, K.V. Sharp, M.M. Mench, J. Electrochem. Soc. 154 (2007) B1295–B1304.
[104] E.C. Kumbur, K.V. Sharp, M.M. Mench, J. Electrochem. Soc. 154 (2007) B1305–B1314.
[105] E.C. Kumbur, K.V. Sharp, M.M. Mench, J. Electrochem. Soc. 154 (2007) B1315–B1324.
[106] A.A. Franco, P. Schott, C. Jallut, B. Maschke, Fuel Cells 7 (2) (2007) 99–117.
[107] M. Inaba, M. Uno, J. Maruyama, A. Tasaka, K. Katakura, Z. Ogumi, J. Electroanal. Chem. 417 (1–2) (1996) 105–111.
[108] M. Andersson, J. Yuan, B. Sunden, Appl. Energy 87 (5) (2010) 1461–1476.
[109] S. Chen, G.D. Doolen, A. R. Fluid Mech. 30 (1) (1998) 329–364.
[110] L.P. Kadanoff, Phys. Today 39 (2) (1986) 6.
[111] S. Succi, The Lattice Boltzmann Equation for Fluid Dynamics and Beyond (Numerical Mathematics and Scientific Computation), Oxford University Press, USA, 2001.
[112] M.C. Sukop, D.T. Throne Jr., Lattice Boltzmann Modeling: An Introduction for Geoscientists and Engineers, Springer–Verlag Berlin Heidelberg, 2007.
[113] J. Park, M. Matsubara, X. Li, J. Power Sources 173 (1) (2007) 404–414.
[114] M.A.A. Spaid, F.R. Phelan Jr., Phys. Fluids 9 (9) (1997) 2468.
[115] M.A. Van Doormaal, J.G. Pharoah, Int. J. Numerical Methods Fluids 59 (1) (2009) 75–89.
[116] F. Higuera, J. Jiménez, Europhys. Lett. 9 (1982) 663–668.
[117] D. Hamilton, A numerical method to determine effective transport coefficients in porous media with application to PEM fuel cells, Masters, Queen's University, 2005.
[118] F.J. Valdes-Parada, J.A. Ochoa-Tapia, J. Alvarez-Ramirez, Phys. A: Stat. Mech. Appl. 388 (6) (2009) 789–798.
[119] J. Park, X. Li, J. Power Sources 178 (2008) 248–257.
[120] G. Karimi, X. Li, J. Power Sources 140 (2005) 1–11.
[121] T. Okada, G. Xie, O. Gorseth, S. Kjelstrup, N. Nikamura, T. Arimura, Electrchem. Acta 43 (1998) 3741–4747.
[122] W. Liu, China Particuol. 3 (6) (2005) 383–394.
[123] B. Lee, K. Cho, Hierarchical multiscale study of metal nanoparticles, 40th Ann. Tech. Meeting of the Soc. of Eng. Sci. Ann Arbor, Mich, 2003.
[124] S. Basu, Recent Trends in Fuel Cell Science and Technology, Asamaya Publishers, New Delhi, 2007.
[125] H.A. Gasteiger, J.E. Panels, S.G. Yan, J. Power Sources 127 (1–2) (2004) 162–171.
[126] N.A. Siddique, F. Liu, Electrochim. Acta 55 (19) (2010) 5357–5366.
[127] K.J. Lange, P.-C. Sui, N. Djilali, J. Power Sources 196 (6) (2011) 3195–3203.
[128] K.J. Lange, P.-C. Sui, N. Djilali, J. Electrochem. Soc. 157 (10) (2010) B1434–B1442.

[129] D. Harvey, J.G. Pharoah, K. Karan, J. Power Sources 179 (1) (2008) 209–219.
[130] Q. Yan, J. Wu, Energy Conv. Mang. 49 (8) (2008) 2425–2433.
[131] S. Um, C.Y. Wang, J. Power Sources 125 (1) (2004) 40–51.
[132] O. Antonio, Y. Bultel, R. Durand, P. Ozil, Electrchem. Acta 43 (24) (1998) 3681.
[133] Y. Bultel, P. Ozil, R. Durand, J. Appl. Electrochem. 28 (1998) 269.
[134] D.M. Bernardi, M.W. Verbrugge, J. Electrochem. Soc. 137 (11) (1990) 3344–3350.
[135] D.M. Bernardi, M.W. Verbrugge, AIChE J. 37 (8) (1991) 1151–1163.
[136] C. Spiegel, PEM Fuel Cell Modeling and Simulation Using Matlab, Academic Press, 2008.